ISSN 1330-3651 (Print), ISSN 1848-6339 (Online) https://doi.org/10.17559/TV-20230623000757
Original scientific paper

Application of Finite Element Analysis for Thermal Cycle Prediction in Butt Welded Plates

Nedeljko VUKOJEVIĆ*, Fuad HADŽIKADUNIĆ, Amna BAJTAREVIĆ-JELEČ

Abstract: The knowledge of the temperature history during the welding process is the crucial first step for understanding the metallurgical and mechanical effects of welding. The present study focused on finite element method for prediction of the thermal cycles induced during three-pass arc welding of butt plates. Two dimensional numerical analysis was performed by taking into account plane at the mid-section of the welded plate. Considering observed welded plates are symmetrical, half of the model was discretized into mesh of rectangular elements with four nodes. The nodal heat quantities were determined according to the real welding parameters and heat inputs were introduced in numerical analysis for defined finite element nodes. The heat flow in the thickness direction was neglected. The finite element model and heat inputs were defined through ANSYS Parametric Design Language code. The thermal analysis boundary condition was defined as convection which was specified using a convection coefficient of $5 \cdot 10^{-6}$ W/mm^{2}K and reference temperature of 25 °C at all nodes. The analysis was carried out for three different finite element models in order to define optimal mesh model. The main difference between observed finite element models is element size and total number of elements. In order to determine the most appropriate finite element model, numerical results of temperature distribution were compared with real experimental values that were measured in transverse direction, during welding process by using thermocouples. Six locations in total, each at varying distances from the weld line, were used as observed points for temperature measuring. The practical application of the used approach was confirmed by establishing that, in the case of all FE models at each observed point, the values of the experimental measurement nearly match the FEA results. The optimal FE model was defined according to cost and time reduction.

Keywords: ANSYS; finite element method; thermal cycles; welding

1 INTRODUCTION

The arc welding process is a very complex phenomenon involving extremely high temperature gradients that cause the non-uniform contraction and expansion of the weld and surrounding base material [1-3]. The differential thermal expansion causes localized plastic deformation in the weld and adjacent regions, and as a result, shrinkage forces are developed in this region during cooling phase. These shrinkage forces could produce residual stresses or distortion in material. The knowledge of the temperature history during the welding process is the essential first step understanding the metallurgical and mechanical aftereffects due to welding. There are various analytical methods for welding temperature prediction. However, most of them are based on many simplifying assumptions that could affect the accuracy of the results.

For the last decades, the finite element method has become the most popular method for both welding thermal cycles and residual stresses prediction. A challenging task for these predictions is determination of appropriate welding heat input model for heat generation. The heat input can be treated as a concentrated heat source which is considered as a normally distributed heat flux on the weld surface [4] or uniformly distributed over the weld volume [5]. Venkatkumar and Ravindran [6] have predicted welding thermal histories using Gaussian surface heat flux distribution of welding arc. However, a major problem associated with this type of heat source is that it tends to provide a less steep temperature gradient ahead of the arc and steeper gradient behind the arc than what was experimentally observed. Tianci Li et al. [7] derived new heat source model for the simulation of residual stress combining Gaussian surface and uniform volume heat source. This model is suitable for welding simulation of T joints because of angled structure. In [8, 9] temperature distribution in submerged arc welding process is predicted using double ellipsoid model of heat source consisting of a combination of two different semi ellipsoidal heat source volumes, proposed by Goldak in [10]. Above mentioned heat source model is proven as convenient model for welding temperature distribution simulation and used in many numerical studies of welding process [11-13]. Proper definition of geometric and energy parameters for the heat calculation is main problem when using Goldak's source. In [11] and [12] mentioned parameters were obtained with the support of the relations found in [14] and [15] respectively. P. Knoedel et al. in [13] defined the values for the parameters as radial dimensions of the molten zone.

Considering the definition of the heat source model requires extreme and accurate calibration phase, G. Ravichandran in [16] proposed simpler procedure based on finite element method for numerical simulation of welding thermal cycles. For this purpose, relations for nodal heat values calculations are proposed. The nodal heat values are introduced in numerical analysis through ANSYS Parametric Design Language code in order to simulate welding heat source. Considering three-dimensional analysis is expensive to perform and time consuming, a two-dimensional analysis can be used in cases where analysis simplification will not affect the accuracy of the results.

The proposed finite element approach [16] is used in the present study to predict the temperature distribution during multi-pass arc welding of butt plates. Since the observed plates are thin, two-dimensional analysis is carried out while neglecting heat flow in the thickness direction.

The results of the numerical calculations using different density of the finite element mesh are compared with conducted experimental results in order to determine optimal finite element model for thermal cycle prediction.

2 NUMERICAL MODELLING AND SIMULATION

2.1 Overview

In the present research, in-plane analysis is carried out by considering the two-dimensional plane at the mid-section of the plate. Only half of the model is taken into account due to symmetry. To perform finite element

analysis, the plate is discretized into mesh of rectangular elements with four nodes.

In order to simulate moving heat source along the length of the plate, the nodal heat values are calculated and assigned to a defined set of nodes. The same nodal heat values are therefore applied to the following set of nodes during the following time step to simulate an arc moving.

The nodal values of heat input are obtained using the following relation:

$$\{F\} = \int q \cdot [N]^T \, \mathrm{d}s \tag{1}$$

The N represents shape function matrix. The arc is assumed to move in the x direction, and the heat flux from the above equation is calculated using relation (2):

$$q(x,y,t) = \frac{3 \cdot \eta \cdot V \cdot I}{\pi \cdot R^2} \cdot \mathrm{e}^{-3 \cdot \frac{[x - v(t-\tau)]^2}{R^2}} \cdot \mathrm{e}^{-3 \cdot \frac{y^2}{R^2}} \tag{2}$$

Considering, the heat is distributed in both x and y directions, the heat input at the four nodes is obtained using double integration with respect to x and y as follows:

$$F_b = \iint q \cdot N_b \mathrm{d}x\mathrm{d}y \tag{3}$$

where b is number of node.

The relations for the shape functions used in the study are given in [16]. The double integration is performed by numerical integration method using Simpson's rule. The distance along x and y is divided into n number of divisions, and h_x and h_y are the values of increments in x and y directions. The heat flux and shape functions are determined for total of $(n + 1)^2$ points of integration. The final integrated value of heat input is obtained as:

$$F = \frac{h_x \cdot h_y}{9} \cdot \sum\sum W_x \cdot W_y \cdot N \cdot q \tag{9}$$

In relation (4) W_x and W_y are weightage factors defined in [16]. The calculations are performed for different time steps.

2.2 Description of the Finite Element Models

The aim of the present study is to determine optimal finite element model for thermal cycle prediction during multi-pass arc welding of two butt plates. The dimensions of the plates are shown in Fig. 1. As mentioned before, due to symmetry, half of model is considered. The arc diameter is defined as 8 mm, according to the recommendations from [16].

The three finite element models with different mesh density are observed in this research. In order to simulate a moving heat arc, the nodal heat input is introduced in the nodes of the first row of elements for models FEM1 and FEM3, and in the nodes of the first and second rows of elements for model FEM2. The dimensions of the above mentioned elements are shown in Fig. 2.

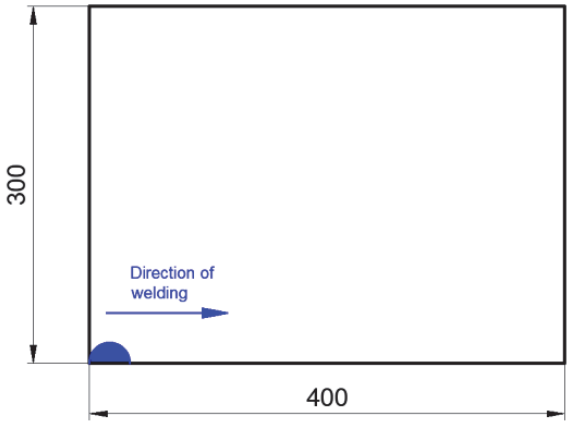

Figure 1 Dimensions of the plate

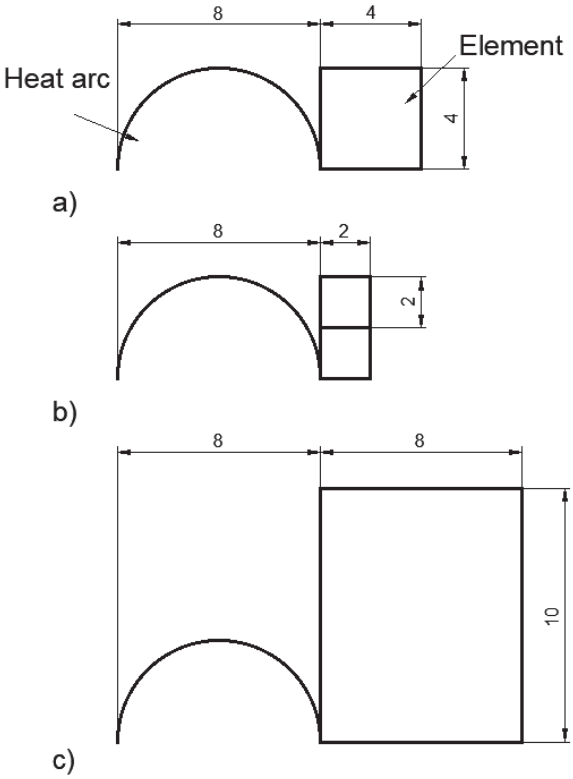

Figure 2 Finite element models: a) FEM1; b) FEM2; c) FEM3

A coarser mesh is defined in the zones farthest from the weld in order to reduce the time of the numerical simulation. In this context, the overall amount of elements and nodes for each model is listed in Tab. 1.

Table 1 Number of elements and nodes of observed models

Model	Total number of elements	Total number of nodes
FEM1	2100	2222
FEM2	13800	14070
FEM3	850	918

2.3 Numerical Approach

The models were created employing the ANSYS Parametric Design Language (APDL) and a direct node generation technique. Two-dimensional four node elements were defined in accordance with the previously generated nodes. Since the transient thermal analysis was performed, it was absolutely essential to employ physical properties of the material corresponding to the temperature

of the specimen during the heating process. Considering the material of observed plates is S235, the material temperature dependent thermal and mechanical properties applied for numerical calculation were extracted from [17] and [18] and shown in Tab. 2.

As a boundary condition of the thermal analysis, the convection was specified using a convection coefficient of $5 \cdot 10^{-6}$W/mm^{2}K and reference temperature of 25 °C at all nodes.

A complete numerical calculations were performed based on APDL commands using ANSYS Mechanical iterative solver.

Table 2 Temperature dependent mechanical and thermal properties of S235

Temperature / °C	Thermal conductivity / W/mmK	Specific heat / J/kgK	Density / kg/mm^3
0	0.065	400	$7.85 \cdot 10^{-6}$
50	0.065	410	$7.85 \cdot 10^{-6}$
250	0.052	500	$7.80 \cdot 10^{-6}$
750	0.03	590	$7.65 \cdot 10^{-6}$
1050	0.022	1300	$7.58 \cdot 10^{-6}$
1250	0.014	610	$7.50 \cdot 10^{-6}$
1450	0.009	610	$7.35 \cdot 10^{-6}$
1600	0.005	500	$7.00 \cdot 10^{-6}$

3 EXPERIMENTAL MEASUREMENTS

The experimental temperature measurements were conducted during butt plate arc welding in order to verify numerical results and select the most appropriate finite element model. Since thickness of plate is 4 mm, welding is performed in three passes. The welding parameters are shown in Tab. 3.

Table 3 Parameters of performed arc welding

Pass	Current / A	Voltage / V	Welding speed / mm/s	Cooling time after pass / s
1	53	25	1.75	153
2	65	26	1.86	210
3	60	26	1.67	500

Cooling times between passes were measured and presented in Tab. 3. During cooling times, arc heat was absent. Cooling was performed at ambient temperature and there was no additional cooling process applied.

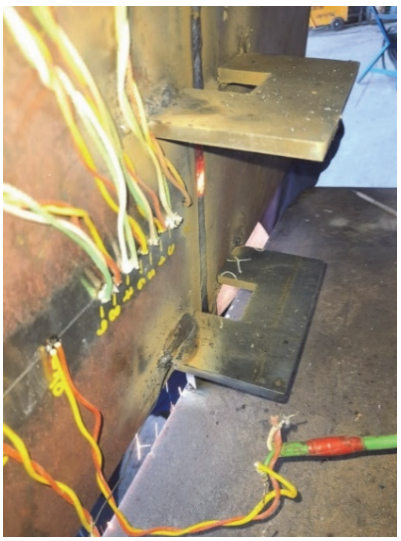

Figure 3 Temperature measurements during welding

The temperature measurements were carried out in transverse direction using thermocouples and automatic attachment unit GTW-V50, at a total of 18 points, as shown in Fig. 3. Due to low thickness of plate, thermocouples were positioned at the opposite of the welding side.

For the purpose of the present study, position of a total of 6 measurement points is adjacent to observed nodes position in numerical simulation. In this respect, position of observed points is shown in Fig. 4.

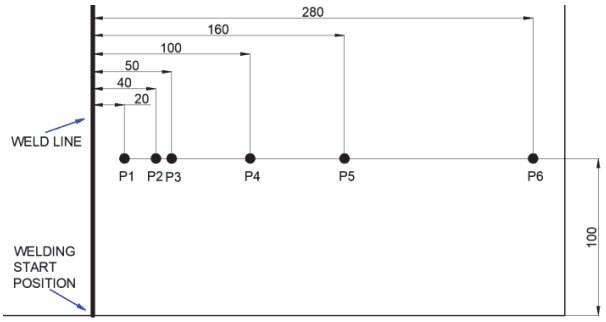

Figure 4 Position of the observed points

4 RESULTS AND DISCUSSION

According to the above presented procedure, the nodal heat inputs were calculated for each described finite element model. The dimensions and parameters used in experimental analysis are applied for generating the numerical models. Since welding was performed in three passes, cooling times between passes were considered into numerical simulation.

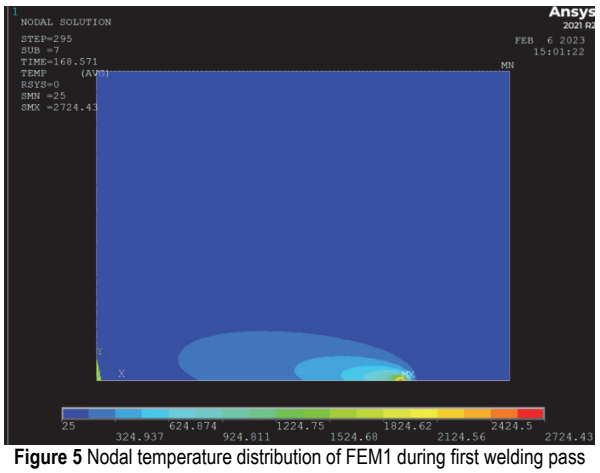

Figure 5 Nodal temperature distribution of FEM1 during first welding pass

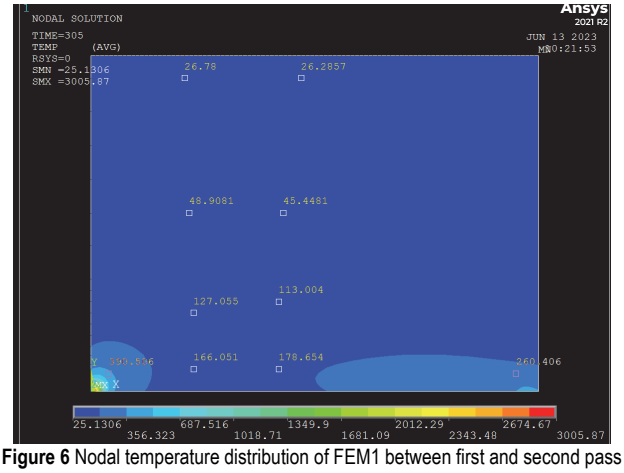

Figure 6 Nodal temperature distribution of FEM1 between first and second pass

Nodal numerical solution of temperature distribution for model FEM1, during first welding pass and between first and second pass is presented in Fig. 5 and Fig. 6, respectively.

Due to different mesh density of models FEM1, FEM2 and FEM3, duration time of numerical simulation significantly differs. In that sense, duration time for FEM1 was about 25 minutes, for FEM2 about 10 hours and for FEM3 about 10 minutes.

The used finite element code is validated using measured experimental results. The comparison between experimental and numerical results of thermal distribution is shown in Figs. 7 to 12. The results are presented for observed points from P1 to P6 in diagrams from Figs. 7 to 12, respectively. Generally, the predicted results are in good agreement with the experimental results. As shown, difference in temperature prediction between used FE models is noticeable. For each pass, the difference between the maximal temperature values measured experimentally and predicted numerically is shown in Tab. 4.

Table 4 Percentage error between experimental and predicted maximum temperature values

FEM/ Pass	P1	P2	P3	P4	P5	P6
1/1	5.6%	13.5%	11.4%	18.4%	25.0%	0.0%
1/2	0.0%	11.0%	17.9%	20.8%	28.6%	9.8%
1/3	10.3%	0.8%	7.1%	11.1%	23.5%	8.9%
2/1	7.9%	25.0%	23.3%	27.3%	30.8%	9.1%
2/2	0.0%	13.6%	20.2%	24.6%	33.3%	15.9%
2/3	13.2%	0.8%	7.1%	12.4%	25.3%	2.1%
3/1	5.3%	15.6%	13.5%	22.5%	33.3%	3.3%
3/2	0.0%	12.4%	22.4%	27.4%	40.0%	13.5%
3/3	7.0%	0.8%	7.6%	14.2%	33.8%	6.1%

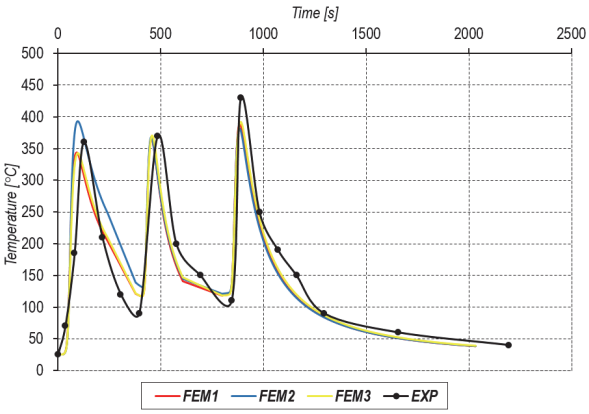

Figure 7 Comparison of FE results with experimental for point P1

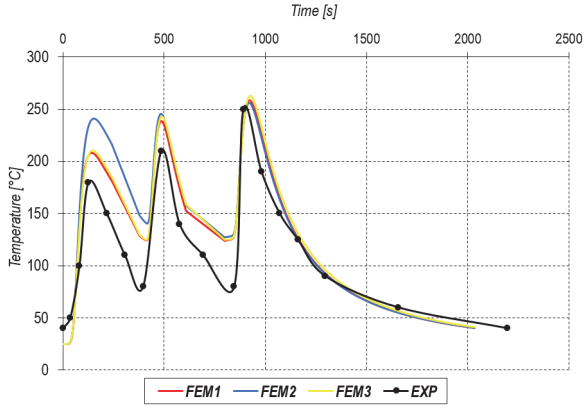

Figure 8 Comparison of FE results with experimental for point P2

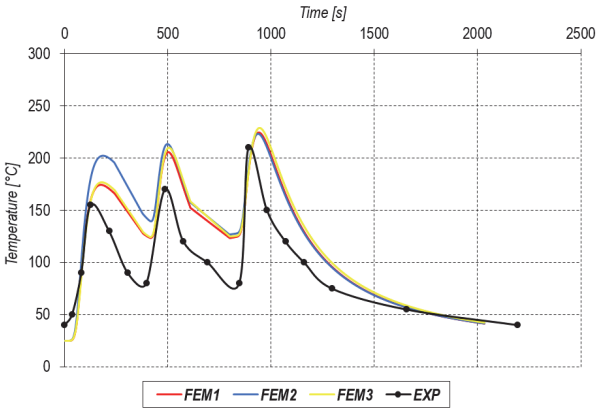

Figure 9 Comparison of FE results with experimental for point P3

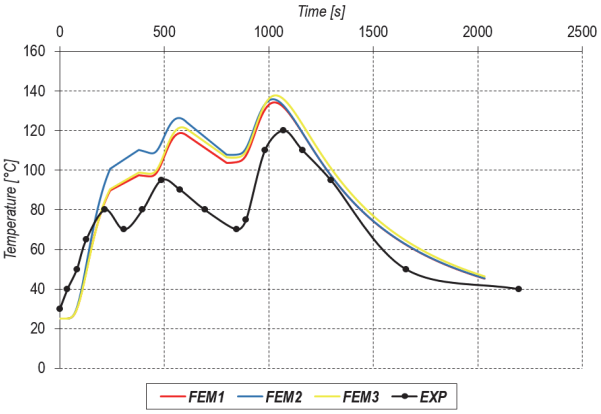

Figure 10 Comparison of FE results with experimental for point P4

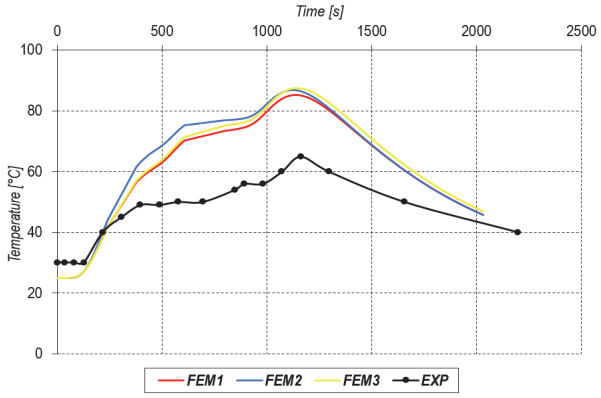

Figure 11 Comparison of FE results with experimental for point P5

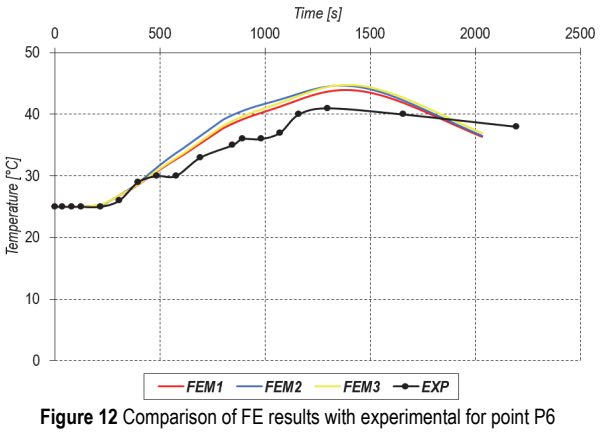

Figure 12 Comparison of FE results with experimental for point P6

The lowest percentage errors were achieved for point 1 (5.3%, 7.0% and 4.1% for FEM1, FEM2 and FEM3, respectively). On the other side, the highest errors were

noticed for point 5 (25.7%, 29.8% and 35.7% for FEM1, FEM2 and FEM3, respectively). Comparison of predicted results percentage deviation between three applied finite element models for each point is presented in Fig. 13.

Evidently, applying finite element model 1 results in the lowest deviation.

Further, it can be noticed that the deviation increases in points away from the weld. Nevertheless, the percentage error for the furthest point is significantly low.

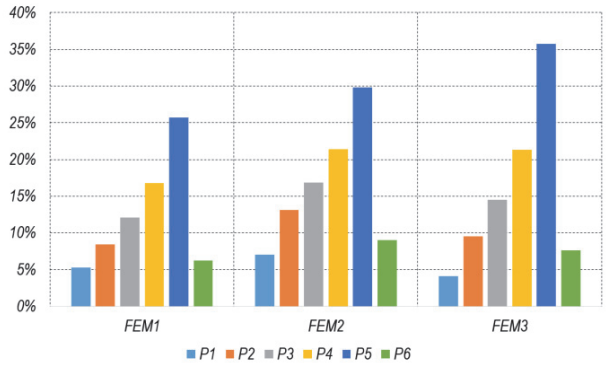

Figure 13 Comparison of percentage error between FE models

5 CONCLUSIONS

The numerical procedure for temperature distribution prediction during multi-pass arc welding of two butt steel plates was developed on the basis of ANSYS APDL subroutine for one-pass welding developed in [16]. For the purpose of determination of optimal FE model for thermal cycle prediction, three FE models with different mesh densities were defined. Numerical calculations were performed using welding parameters applied in conducted experimental welding process.

As demonstrated in the current study, model FEM1 provided the best agreement between predicted and experimental results with average deviation of maximal temperature in amount of 12.4%. The remaining two models' error rates are 15.5% for FEM3 and 16.2% for FEM2.

All numerical calculations were performed using server computer with 10-core CPU and 32 GB of RAM. Due to mesh density, numerical simulation duration times of FEM1 and FEM3 are significantly less compared to model FEM2. The accuracy of FEM1 provides the best finite element model for predicting welding temperature distribution, even though the duration costs are only marginally different compared to FEM3.

As can be seen from the Fig. 13, percentage deviation rises with the distance from the weld line until the last measured point, while the deviation value rapidly decreases. The rise of deviation is expected due to cooling conditions that could not be fully defined in numerical simulation. The welding was performed in a production hall rather than a lab, where it was impossible to properly control conditions like air flow and temperature variations.

On the other hand, due to the point's distant location from the weld bed, plate variations in temperature at point 6 were minimal, as shown in Fig. 12. For that reason, percentage deviation between numerical and experimental results is low.

Industrial Applicability

Given that this research confirmed the effectiveness of the approach for predicting welding thermal fields, it is possible that the method will be useful for predicting temperatures during welding and cooling of thin industrial structures. Numerical calculation of temperatures is based on real welding parameters. The costly and time-consuming experimental temperature measurements during welding may be replaced by numerical calculation of temperature fields. Thus, using numerical methods is cost-effective and time-efficient.

Temperature measurements at the weld region and the vicinity of the weld line, which are impossible to get using experimental measuring tools like thermocouples, may also be made using the numerical technique. Furthermore, unlike other approaches, numerical prediction provides a temperature history for the whole structure from the beginning of welding to the end of cooling. Then, temperature histories might be used for additional research on residual stress and weld quality of industrial structures. This research also confirms that numerical method is applicable for multi-pass arc welding.

6 REFERENCES

[1] Yang, L., Yang, B., Yang, G. W., Xiao, S. N., Zhu, T., & Wang, F. (2022). Fatigue-Life Evaluation Method for Ring-Welded Joints. *International Journal of Simulation Modelling*, *21*(2), 320-331. https://doi.org/10.2507/IJSIMM21-2-CO6

[2] Zhou, Q. H., Zhu, X. Y., Sun, J. M., & Li, J. (2022). Control of Welding Residual Stress and Deformation for the Rod Support of a Crane. *International Journal of Simulation Modelling*, *21*(3), 501-512. https://doi.org/10.2507/IJSIMM21-3-CO12

[3] Yang, L., Yang, B., Yang, G.W., Xiao, S. N., Zhu, T., & Wang, F. (2022). A method for prediction of S-N curve of spot-welded joints based on numerical simulation, *Advances in Production Engineering & Management*, *17*(2), 141-151. https://doi.org/10.14743/apem2022.2.426

[4] Mondal, A. K., Lohit, A., Biswas, P., Bag, S., & Das, M. (2016). Prediction of weld-induced distortion of large structure using equivalent load technique. *Proceedings of the Institution of Mechanical Engineers, Part B: Journal of Engineering Manufacture*, *232*(3), 499-512. https://doi.org/10.1177/0954405416646309

[5] Perić, M., Nižetić, S., Tonković, Z., Garašić, I., Horvat, I., & Boras, I. (2020). Numerical Simulation and Experimental Investigation of Temperature and Residual Stress Distributions in a Circular Patch Welded Structure. *Energies*, *13*(20), 5423. https://doi.org/10.3390/en13205423

[6] Venkatkumar, D. & Ravindran, D. (2019). Effect of Boundary Conditions on Residual Stresses and Distortion in 316 Stainless Steel Butt Welded Plate. *High Temperature Materials and Processes*, *38*(2019), 827-836. https://doi.org/10.1515/htmp-2019-0048

[7] Li, T., Zhang, L., Chang, C., & Wei, L. (2018). A Uniform-Gaussian distributed heat source model for analysis of residual stress field of S355 steel T welding. *Advances in Engineering Software*, *126*, 1-8. https://doi.org/10.1016/j.advengsoft.2018.09.003

[8] Arora, H., Singh, R., & Brar, G. S. (2019). Prediction of Temperature Distribution and Displacement of Carbon Steel Plates by FEM. *Materials Today: Proceedings*. https://doi.org/10.1016/j.matpr.2019.07.264

[9] Negi, V. & Chattopadhyaya, S. (2013). Critical Assessment of Temperature Distribution in Submerged Arc Welding

Process. *Advances in Materials Science and Engineering, 2013*, 1-9. https://doi.org/10.1155/2013/543594
[10] Goldak, J., Chakravarti, A. P., & Bibby, M. (1984). A new finite element model for welding heat sources. *Metallurgical Transactions. A, Physical Metallurgy and Materials Science*, *15*(2), 299-305. https://doi.org/10.1007/bf02667333
[11] Prasad, V. R., Varghese, V., Suresh, M., & Kumar, D. S. (2016). 3D Simulation of Residual Stress Developed During TIG Welding of Stainless Steel Pipes. *Procedia Technology*, *24*, 364-371. https://doi.org/10.1016/j.protcy.2016.05.049
[12] Guimarães, P. B., Pedrosa, P., Yadava, Y. P., Barbosa, J. C., Filho, A. B., & Ferreira, R. B. (2013). Determination of Residual Stresses Numerically Obtained in ASTM AH36 Steel Welded by TIG Process. *Materials Sciences and Applications*, *04*(04), 268-274. https://doi.org/10.4236/msa.2013.44033
[13] Knoedel, P., Gkatzogiannis, S., & Ummenhofer, T. (2017). Practical aspects of welding residual stress simulation. *Journal of Constructional Steel Research*, *132*, 83-96. https://doi.org/10.1016/j.jcsr.2017.01.010
[14] Deng, D. & Murakawa, H. (2006). Numerical simulation of temperature field and residual stress in multi-pass welds in stainless steel pipe and comparison with experimental measurements. *Computational Materials Science*, *37*(3), 269-277. https://doi.org/10.1016/j.commatsci.2005.07.007
[15] Gery, D., Long, H., & Maropoulos, P. (2005). Effects of welding speed, energy input and heat source distribution on temperature variations in butt joint welding. *Journal of Materials Processing Technology*, *167*(2-3), 393-401. https://doi.org/10.1016/j.jmatprotec.2005.06.018
[16] Ravichandran, G. (2020). *Finite Element Analysis of Weld Thermal Cycles Using ANSYS (1st ed.)*. CRC Press. https://doi.org/10.1201/9781003052128
[17] Pfeiler, C. (2008). Modeling of Turbulent Particle/Gas Dispersion in the Mold Region and Particle Entrapment into the Solid Shell of a Steel Continuous Caster. https://pure.unileoben.ac.at/en/publications/modeling-of-turbulent-particlegas-dispersion-in-the-mold-region-a
[18] Miłkowska-Piszczek, K. & Korolczuk-Hejnak, M. (2013). An Analysis of The Influence of Viscosity on The Numerical Simulation of Temperature Distribution, as Demonstrated by the CC Process. *Archives of Metallurgy and Materials*, *58*(4), 1267-1274. https://doi.org/10.2478/amm-2013-0146

Contact information:

Nedeljko VUKOJEVIĆ, Professor
(Corresponding author)
University of Zenica,
Faculty of Mechanical Engineering,
Fakultetska 1, 72000 Zenica, Bosna I Hercegovina
E-mail: nedeljko.vukojevic@unze.ba

Fuad HADŽIKADUNIĆ, Professor
University of Zenica,
Faculty of Mechanical Engineering,
Fakultetska 1, 72000 Zenica, Bosna I Hercegovina
E-mail: fuad.hadzikadunic@unze.ba

Amna BAJTAREVIĆ-JELEČ, Teaching Assistant
University of Zenica,
Faculty of Mechanical Engineering,
Fakultetska 1, 72000 Zenica, Bosna I Hercegovina
E-mail: amna.bajtarevic@unze.ba